Impact of climate change on the blue water footprint of agriculture on a regional scale

Huiping Huang, Yuping Han and Dongdong Jia

ABSTRACT

In the case study of Tangshan city, Hebei Province, China, this paper analyzes the temporal change of the blue agricultural water footprint (WF) during 1991–2016 and discusses the applicability of different climate change models during 2017–2050. Results show effective rainfall, wind speed and maximum temperature are leading factors influencing the blue agricultural WF. Relative error analysis indicates that the HadGEM2-ES model is the most applicable for climate change projections in the period of 2017–2050. Agricultural blue WF is about 1.8 billion m^3 in RCP2.6, RCP4.5 and RCP8.5 emission scenarios, which is almost equal to the average value during 1991–2016.

Key words | agricultural blue WF, climate change, CMIP5 model, emission scenario, partial least squares regression (PLSR)

Huiping Huang
Yuping Han (corresponding author)
Dongdong Jia
North China University of Water Resources and
    Electric Power,
Zhengzhou 450045,
China
E-mail: han0118@163.com

Huiping Huang
Collaborative Innovation Center of Water
    Resources Efficient Utilization and Support
    Engineering,
Zhengzhou 450046,
China

Yuping Han
Henan Key Laboratory of Water Environment
    Simulation and Treatment,
Zhengzhou 450046,
China

INTRODUCTION

Due to the uneven distribution of water at spatial and temporal scales, more than two billion people live in water-stressed areas (Oki & Kanae 2006). Simulations have shown that 59% of the world's population will face water shortage by 2050 (Rockström et al. 2009). Agricultural water use currently accounts for ~70% of freshwater withdrawals both globally and in China. The water footprint (WF) of a product was first defined in 2003 as the volume of freshwater used for production at the place where the product is actually produced (Hoekstra & Hung 2002) and it consists of green WF, blue WF, and grey WF. In this paper, grey WF is not considered in the WF calculation for crops. Green WF is defined as rainwater consumption that is stored in soil and evaporated during production during crop growth. Blue WF refers to surface and groundwater that is consumed by irrigation and evaporated, and

the agricultural blue WF is considered as the theoretical irrigation water requirement.

Climate change is a global issue that may have dramatic impacts on ecosystems, social economics, and agriculture. Changes in the availability of water, particularly for agriculture, due to climate change have been observed and reported globally (Burn & Hesch 2007). Temperature increase and precipitation decrease in the Zayandeh–Rud River Basin is expected to cause increasing irrigation water demand from 2015 to 2055 (Gohari et al. 2013). Based on crop data and changes in the seasonal timing of water demand, irrigation water requirements in the Guadalquivir River Basin of Spain are projected to increase 15%–20% by the 2050s (Rodríguez-Díaz et al. 2007). The satellite weather application platform (SWAP) model, global change models (GCM), and regional climate models (RCM) have been used to predict local impacts of climate change on irrigation water demand in Turkey (Yano et al. 2007). The expected water requirements of global irrigation, without measures to alleviate climate change impacts, may increase ~20% by

2080 (Fischer *et al.* 2007). The impacts of climate change on agricultural water use, especially on irrigation water demand, have been reported in numerous studies in China (Zhang & Cai 2013). Existing studies have shown that the influence of climate change on regional irrigation water demand varies greatly among different areas (Zang *et al.* 2013; Wang *et al.* 2016). Research on the effects of climate change on the agricultural blue WF is of great significance for guiding agricultural management to cope with climate change.

At present the climate change model is the main approach to predicting future climate and its associated human response. However, initial and boundary conditions, scenarios, observations, model parameters, and structure of climate simulations all cause some degree of uncertainty in simulation results, and uncertainty is more prominent at the regional scale (IPCC 2013; Knutti & Sedláček 2013). Therefore, evaluating the adaptability of climate change models to different regions is essential for climate change model use.

The main objectives of this paper were to: (1) identify key meteorological variables influencing the blue WF of major crops and calculate the relative error of these variables with different climate change models during 1991–2016; and (2) determine an applicable model for a specific region and use it to calculate the WF in 2017–2050. The results will help guide regional water use management.

MATERIALS AND METHODS

Site description and data

Located in the east of Hebei, a province in north China, Tangshan covers an area of ~13,472 km^2 (Figure 1). The city is characterized by a typical mainland monsoon climate with annual precipitation of 644.2 mm. The per capita water resources in Tangshan are 329 m^3, which are less than 15% of that in China and water resources in the region are in short supply. Agricultural water consumption accounts for about 60% of the total regional water use and crop irrigation water takes up more than 90% in this region.

Daily meteorological data from 1991 to 2016 were acquired from the China Meteorological Data Service Center (http://data.cma.cn/). Parameters included average

air temperature, average relative humidity, average wind speed, sunshine hours, and precipitation. Time series of crop yield were taken from annals of statistics for Tangshan. Data from the coupled model inter-comparison project phase 5 (CMIP5) released by the Earth System Grid Federation were downloaded from the internet with a grid distance of 25 km, and data used in calculations were interpolated to 0.5 degrees with a bilinear interpolation method.

Methods

Agricultural blue WF

The green and blue WF of primary crops can be calculated with the following equations (Hoekstra & Chapagain 2007):

$$WF_{\text{green}} = \frac{CWU_{\text{green}}}{Y} = 10 \times \frac{ET_{\text{green}}}{Y}$$
$$WF_{\text{blue}} = \frac{CWU_{\text{blue}}}{Y} = 10 \times \frac{ET_{\text{blue}}}{Y} \tag{1}$$

where WF_{green} is a crop's green WF (m^3/kg), WF_{blue} is the blue WF (m^3/kg), CWU_{green} and CWU_{blue} are green and blue water consumption (m^3/ha), 10 is a constant to convert water depth (mm) into water volume (m^3/ha), and Y is crop yield (m^3/ha).

For a certain type of crop in an irrigation district, consumption of green and blue water for the crop's water requirements during the entire growth period is (Novo *et al.* 2009):

$$ET_{\text{g}}[c, q, m] = \min (CWR[c, q, m], P_{\text{eff}}[q, m])$$
$$ET_{\text{b}}[c, q, m] = \max (0, CWR[c, q, m] - ET_{\text{g}}[c, q, m]) \tag{2}$$
$$CWU_{\text{b}}[c, q, t] = \sum_{m=1}^{t} ET_{\text{b}}[c, q, m])$$

where c stands for crop type, q represents area, $ET_{\text{g}}[c,q,m]$ and $ET_{\text{b}}[c,q,m]$ are the green and blue water of the mth month, CWR is the crop water requirement, P_{eff} is effective precipitation, and $CWU_{\text{b}}[c,q,t]$ is the blue water requirement of the tth month, which directly reflects the theoretical need for irrigation.

During computation, the CWR is assumed to be equal to crop evapotranspiration (ET_{c}, mm/day), which can be calculated by multiplying the potential reference evapotranspiration (ET_0, mm/day) and the crop coefficient (K_{c}).
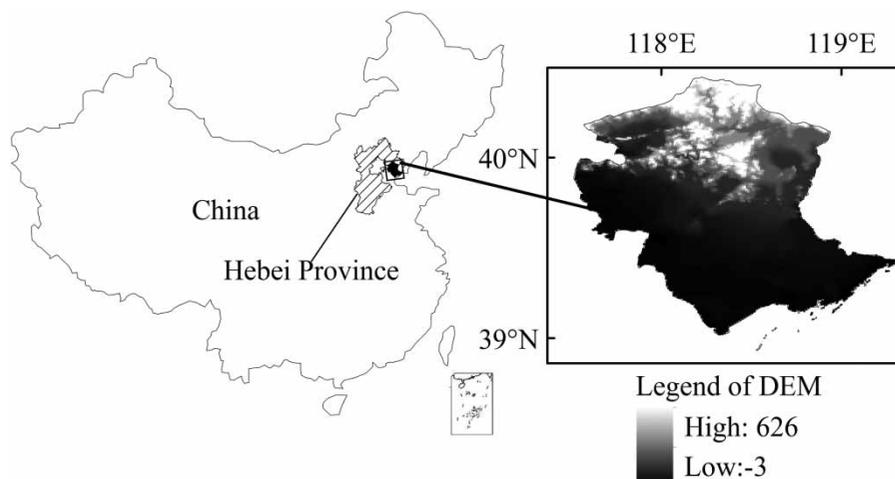
Figure 1 | Location of Tangshan city in China.

In this study, ET_0 was calculated using the Penman–Monteith equation recommended by the FAO in 1998. The parameter K_c is obtained based on current values in Tangshan City and Hebei Province combined with parameters from FAO-56.

Meteorological yield

Crop yield in any given year is strongly influenced by at least three kinds of factors: meteorological variability, agricultural economic practice, and random noise. Briefly, crop yield can be decomposed as

$$y = y_t + y_w + \Delta y \tag{3}$$

where y represents crop yield, y_t denotes trend yield (mainly determined by social productivity), y_w is meteorological yield (mainly determined by climatic conditions), and Δy stands for the yield component produced by random elements that can be ignored in the actual calculation.

RESULTS AND DISCUSSION

Applicability of climate change model

Agricultural WF in Tangshan

In Tangshan, the main cultivated crops include soybeans, sorghum, oil crops, cotton, vegetables, tubers, muskmelon, watermelon, winter wheat, tobacco, summer maize, and rice. Among the 12 kinds of crops, the WF of summer maize, winter wheat, oil crops, cotton, vegetables, and rice accounted for more than 94% of the entire agricultural WF of the city. Therefore, to simplify other analyses in this paper, these six crops were selected to represent the major crops of Tangshan.

Agricultural blue WF

The agricultural blue WF is closely related to CWR and effective precipitation, which reflect the combined effect of growth period, precipitation, topography, and meteorological conditions. In Tangshan city, the WF of summer maize is the highest, followed by winter wheat; however, the blue WF of winter wheat exceeds that of summer maize because the growth period of summer maize is consistent with the rainy season (June–September), which makes it possible for some of its water requirement to be satisfied by green water.

The total blue WF displayed an insignificant downward trend of -0.27 billion m^3 per decade from 1991 to 2016, which is favorable to the current water crisis. The blue WF showed strong annual fluctuations because it was affected by meteorological variables, especially precipitation, which had strong annual variations. According to specific crops, the blue WF of winter wheat and rice (significantly) and of summer maize and oil crops (insignificantly) decreased, whereas that of vegetables and cotton increased significantly. The total volume of the blue WF was between

1.17 billion m^3 and 2.82 billion m^3, with an average value of 1.79 billion m^3. The volume of the blue WF for grain crops including winter wheat, summer maize, and rice was 80% of that for the whole region. Therefore, reducing the irrigation water demand for these three types of crops is critical for water conservation.

Simulation accuracy of meteorological factors with different climate models

Although climate projection is an important tool for understanding and estimating past and future climate change and has been widely used in agriculture, environmental science, and ecology, previous studies have suggested that uncertainty exists in the simulation of meteorological factors, especially precipitation (Boberg *et al.* 2010). Therefore, it is necessary to analyze the applicability of climate models in specific areas. Accurate simulation of the dominant factors impacting blue WF (effective precipitation, wind speed,

and maximum temperature) is important for estimating the applicability of climate models. The climate models used in this paper include GFDL-ESM2M, HadGEM2-ES, IPSL-CM5A-LR, MIROC-ESM-CHEM, and NorESM1-M of CMIP5, which are relatively applicable in China. Relative error was employed to determine the simulation accuracy of the five models:

$$RE = Relative\ error = \frac{x_{\text{sim}} - x_{\text{obs}}}{x_{\text{obs}}}$$

$$TE = Total\ error = \sum_{i=1}^{n} |RE| \times p_i \tag{4}$$

where RE is the relative error of climatic parameters, x_{sim} is simulated multi-year average data, x_{obs} is mean annual measured data, TE is the total error of climatic parameters, and p_i is the proportion of total blue WF for winter wheat, summer maize, rice, cotton, oil crops, and vegetables, respectively. The results are shown in Table 1 ((a)–(e)).

Table 1 | Relative error of different climate models

	RE						TE
	Winter wheat	Summer maize	Rice	Cotton	Oil crops	Vegetables	
(a) GFDL-ESM2M model							
Effective precipitation	6.21	3.95	3.51	4.36	3.95	2.93	4.59
Wind speed	5.49	12.88	4.87	5.50	1.29	−1.63	7.2
Maximum temperature	−1.20	−0.87	−1.11	−1.19	−0.87	−1.29	1.07
(b) HadGEM2-ES model							
Effective precipitation	5.01	2. 52	2.55	3.67	2.52	4.29	3.57
Wind speed	3.72	6.44	7.14	6.32	16.44	−3.17	5.95
Maximum temperature	−1.18	−0.66	−0.43	−0.86	−0.66	−0.84	0.87
(c) IPSL-CM5A-LR model							
Effective precipitation	9.33	1. 36	3.77	3.87	1.36	5.01	4.85
Wind speed	7.79	7.71	3.21	3.74	7.71	−1.07	6.33
Maximum temperature	−1.66	0	−0.68	−0.57	0	−1.33	0.83
(d) MIROC-ESM-CHEM model							
Effective precipitation	9.70	4.16	3.27	5.67	4.16	6.82	6.2
Wind speed	29.44	6.22	2.80	37.49	6.22	43.83	18.17
Maximum temperature	−1.05	−0.56	−0.40	−0.56	−0.56	−6.90	1.21
(e) NorESM1-M model							
Effective precipitation	9.03	2.18	3.27	4.60	2.58	5.15	5.06
Wind speed	6.40	10.12	3.01	4.20	10.12	−2.64	6.89
Maximum temperature	−1.35	−0.83	−0.97	−1.00	−0.83	−1.40	1.08

Among the three meteorological factors, the simulation error of maximum temperature produced by the five climate models was the lowest and that of wind speed was the highest. The relative error of wind speed produced by the MIROC-ESM-CHEM model during the growth periods of winter wheat, cotton, and vegetables reached up to 29.44%, 37.49%, and 43.83%, respectively, indicating that the MIROC-ESM-CHEM model is not suitable for Tangshan climate projection. Effective precipitation was the most important influential factor and had a strong impact on the blue WF of winter wheat, summer maize, and rice; the combined blue WF of these crops accounted for 81% of the regional blue WF. The second most important influential factor was wind speed, followed by maximum temperature. Table 1 shows that the TE values for effective precipitation and wind speed in HadGEM2-ES were 3.57 and 5.95 respectively, which correspond to the minimum error for the five models. The minimum TE for maximum temperature was 0.8 in the IPSL-CM5A-LR model. Therefore, the HadGEM2-ES model is considered most suitable for climate simulations of blue WF in Tangshan.

CWR under different future climate change scenarios

Three representative concentration pathway (RCP) scenarios (RCP2.6, RCP4.5, and RCP8.5) were considered for projections of future CWR conditions in Tangshan. The projected average annual CWR for winter wheat under climate scenarios from 2017 to 2050 was 488.02 mm, 512.31 mm, and 510.01 mm, respectively, smaller than the average value of 520.92 mm during 1991–2016 (Figure 2). Data from these three climate scenarios showed a significant upward trend (99% confidence level), opposite to the trend during 1991–2016. The CWR for summer maize increased significantly (99% confidence level) under the three scenarios, with average values of 477.09 mm, 485.92 mm and 494.39 mm, respectively. Values in RCP4.5 and RCP8.5 were bigger than the average value of 479.14 mm. The respective average water requirements of rice under the three scenarios were 852.61 mm, 861.30 mm, and 876.98 mm, which vary largely from the average value of 749.36 mm during 1991–2016. In comparison with average data from 1991 to 2016, the projected CWR for cotton, oil crops, and vegetables were all larger
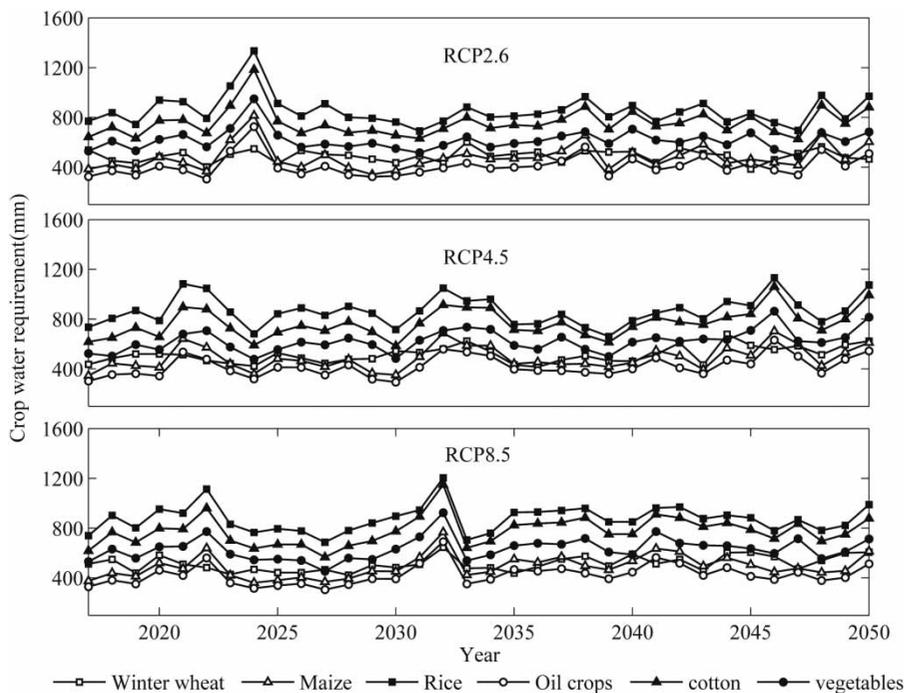

Figure 2 | CWR of crops from 2017 to 2050.

in 2017–2050. Accordingly, climate change may cause crop requirements to rise in the future.

Crop yields under climate change

Assessment of PLSR predictive results

Yield data from 1991 to 2010 were decomposed into trend yield and meteorological yield using a linear moving average method with 5-year moving windows. Results of the path analysis indicate that temperature difference, sunshine hours, and precipitation sufficiently reflect the influence of climatic factors on crop yield. These three meteorological factors were selected as dependent variables for the partial least squares regression (PLSR) model, with meteorological yield as the independent variable. The PLSR model was established using meteorological crop yield and average meteorological data from different growth periods. The sum of trend yield and simulated meteorological yield were considered as the simulated annual yield. Actual yield data from 2011 to 2016 were used to assess the simulation accuracy of different types

of crops. Error for the six types of crops was all below 10%; thus, the PLSR model is suitable for crop yield prediction.

Crop yields under climate change

The corrected projection data and PLSR were used to simulate crop yield during 2017–2050. With the exception of winter wheat in all scenarios and summer maize in RCP2.6, the yield of all crops decreased. For winter wheat, summer maize, rice, and cotton, both yield gains and losses were highest under RCP8.5 and lowest under RCP2.6. The largest decrease in oil crop output occurred under the RCP4.5 scenario. The yield of winter wheat was almost the same under all scenarios; rice yield in RCP2.6 increased by 900 kg/ha compared with that in RCP4.5 and RCP8.5. No obvious changes in the yield of other crops were evident, showing that the influence of climate change on yield varies among crops.

Agricultural WF in 2017–2050

Figure 3 shows the WF and blue WF of crops under RCP2.6, RCP 4.5, and RCP8.5 scenarios over the period of
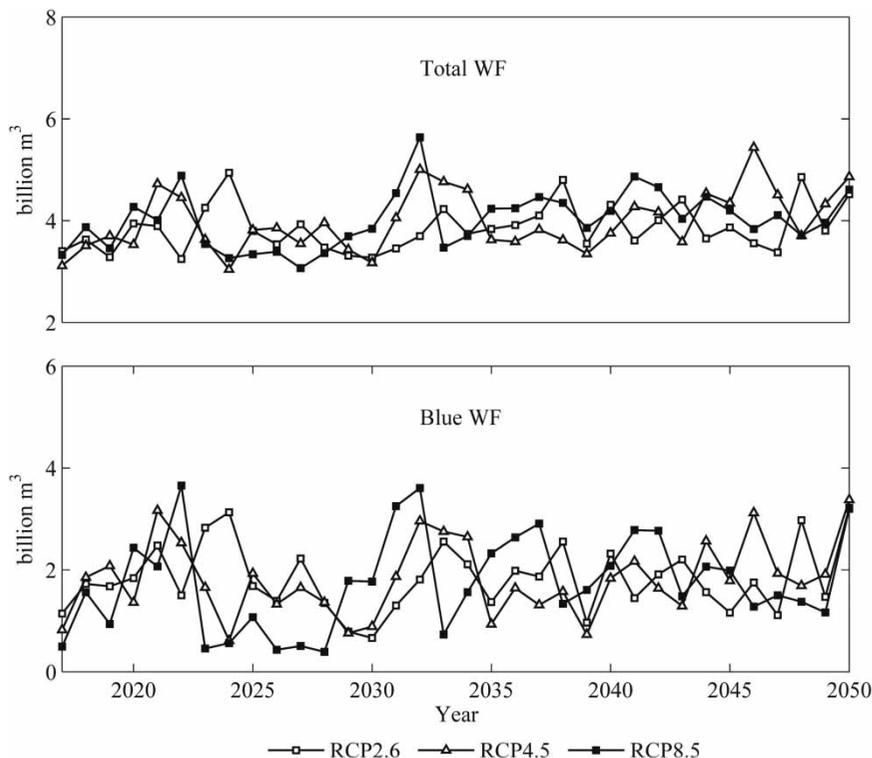

Figure 3 | WF of crops from 2017 to 2050 under three climate change scenarios.

2017–2050. The predicted average footprint during 2017–2050 under RCP2.6, RCP 4.5, and RCP8.5 was 3.85 billion m^3, 3.97 billion m^3, and 4.02 billion m^3 and the blue WF was 1.85 billion m^3, 1.81 billion m^3, and 1.83 billion m^3, respectively, almost equal to the average value during 1991–2016. The WF and blue WF varied slightly among the three emission scenarios because of different impacts of climate change on crop water requirement and crop yield.

Implications of water resources management

As discussed in this paper, reducing winter wheat and summer maize yield can have a large impact on regional blue WF. In contrast, significant increases in vegetables cause only small changes to the regional blue WF. This is because the blue WF per unit mass of vegetables is only 14.72 m^3/ton, whereas that of winter wheat and summer maize is 846.4 and 407.8 m^3/ton, respectively. Therefore, adjustments to planting structure can be implemented to mitigate water scarcity. Tangshan city should plant more vegetables and limit wheat planting. In addition, an interregional virtual water compensation scheme can provide a practical solution for water shortages.

CONCLUSIONS

In this paper, we presented a comprehensive analysis of the effects of climate change on regional agricultural blue WF based on meteorological and economic data, using the city of Tangshan as an example. Winter wheat, summer maize, rice, cotton, oil crops, and vegetables account for 94% of the total agricultural WF, and blue WF contributes 53.08% of the total agricultural WF. This demonstrates that these six crop varieties are major factors in the regional agricultural water resources system. Effective precipitation, wind speed, and maximum temperature are the main factors impacting the agricultural blue WF. The HadGEM2-ES model has the minimum total error for 2017–2050 simulations, and thus was selected as the most applicable climate change model. PLSR model simulations were used to calculate the blue WF of six kinds of crops under RCP2.6, RCP4.5, and RCP8.5 emission scenarios. The results showed that average agricultural blue WF during

2017–2050 varied slightly compared with that during 1991–2016 because of the inverse effect of climate change on crop water requirement and yield.

The methods used in this paper provide an example of agricultural blue WF simulations in a specific region and can be used to guide management of water resources. However, there are some limitations of the method used in this paper. Firstly we analyzed only five climate change models, and more models should be investigated in future research. In addition, the same climatic parameters were used in the analysis of the simulation accuracy of climate change models, but the factors influencing blue WF are different for the studied crops and should be explored individually. Further studies should be implemented to address the limitations listed above to achieve more accurate predictions of blue WF.

ACKNOWLEDGEMENTS

REFERENCES

Boberg, F., Berg, P., Thejll, P., Gutowski, W. J. & Christensen, J. H. 2010 Improved confidence in climate change projections of precipitation further evaluated using daily statistics from ENSEMBLES models. *Climate Dynamics* **35** (7–8), 1509–1520.

Burn, D. H. & Hesch, N. M. 2007 Trends in evaporation for the Canadian Prairies. *Journal of Hydrology* **336** (1–2), 61–73.

Fischer, G., Tubiello, F. N., van Velthuizen, H. & Wiberg, D. A. 2007 Climate change impacts on irrigation water requirements: effects of mitigation, 1990–2080. *Technological Forecasting and Social Change* **74** (7), 1083–1107.

Gohari, A., Eslamian, S., Abedi-Koupaei, J., Bavani, A. M., Wang, D. B. & Madani, K. 2013 Climate change impacts on crop production in Iran's Zayandeh-Rud River Basin. *Science of the Total Environment* **442**, 405–419.

Hoekstra, A. Y. & Chapagain, A. K. 2007 Water footprints of nations: water use by people as a function of their consumption pattern. *Water Resources Management* **21** (1), 35–48.

Hoekstra, A. Y. & Hung, P. Q. 2002 *Virtual Water Trade: A Quantification of Virtual Water Flows between Nations in Relation to International Crop Trade*, Value of Water Research Report Series No. 11. UNESCO-IHE, Delft, The Netherlands, pp. 92–103.

IPCC 2013 *Climate Change 2013: The Physical Science Basis. Contribution of Working Group I to the Fifth Assessment Report of the Intergovernmental Panel on Climate Change.* Cambridge University Press, Cambridge, UK.

Knutti, R. & Sedláček, J. 2013 Robustness and uncertainties in the new CMIP5 climate model projections. *Nature* **3**, 369–373.

Novo, P., Garrido, A. & Varela-Ortega, C. 2009 Are virtual water 'flows' in Spanish grain trade consistent with relative water scarcity? *Ecological Economics* **68** (5), 1454–1464.

Oki, T. & Kanae, S. 2006 Global hydrological cycles and world water resources. *Science* **313**, 1068–1072.

Rockström, J., Falkenmark, M., Karlberg, L., Hoff, H., Rost, S. & Gerten, D. 2009 Future water availability for global food production: the potential of green water for increasing resilience to global change. *Water Resources Research* **45**, W00A12. doi:10.1029/2007WR006767.

Rodríguez-Díaz, J. A., Weatherhead, E. K., Knox, J. W. & Camacho, E. 2007 Climate change impacts on irrigation water requirements in the Guadalquivir river basin in Spain. *Regional Environmental Change* **7** (3), 149–159.

Wang, X. J., Zhang, J. Y., Ali, M., Shahid, S., He, R. M., Xia, X. H. & Jiang, Z. 2016 Impact of climate change on regional irrigation water demand in Baojixia irrigation district of China. *Mitigation and Adaption Strategies for Global Change* **21**, 233–247.

Yano, T., Aydin, M. & Haraguchi, T. 2007 Impact of climate change on irrigation demand and crop growth in a Mediterranean environment of Turkey. *Sensors* **7**, 2297–2315.

Zang, C., Liu, J., Jiang, L. & Gerten, D. 2013 Impacts of human activities and climate variability on green and blue water flows in the Heihe River Basin in Northwest China. *Hydrology and Earth System Science* **10**, 9477–9504.

Zhang, X. & Cai, X. M. 2013 Climate change impacts on global agriculture water deficit. *Geophysical Research Letters* **40** (6), 1111–1117. doi:10.1002/grl.50279.